FLD GURSON FÉMMEL EGYSZERŰ LAPOS MINTÁHOZ

FLD WITH GURSON METAL FOR SIMPLE FLAT SPECIMEN

Domokos Tatiane, Baksa Atilla**, Szávai Szabolcs****

ABSTRACT

In the past, the prediction of ductile damage and fracture of metal materials under complex loadings has been an important topic in industries like the metal forming industry. The GTN model is one of the most classical damage models regarding damage mechanics, which has a wide application and perfect evolution in studies of fracture of ductile metal. GTN originated from Gurson and later enhanced by Tvergaard and Needleman. The improvement consists of inserting an equivalent void volume fraction f and two more parameters called q_1 and q_2 into the yield function of Gurson's model, to model the complete loss of load-carrying capacity at a realistic void volume fraction.

Keywords: Forming limit diagram (FLD); Gurson model; Abaqus

1. INTRODUCTION

This paper presents a short explanation about the Forming Limit Diagram (FLD) and the GTN model. It gives the result of simulations of a simple flat specimen by means of the Abaqus simulation software. The test result is for a flat specimen based on the deformation and fracture of tensile test. The material simulated here is Aluminum alloy 6061. The goal of this work is to start a study where a forming limit diagram and the desired material characterization will be determined, intended for the metal forming industry. Finally, the GTN parameters can be determined based on some experiments on a simple specimen.

2. FORMING LIMIT DIAGRAM (FLD)

A forming limit diagram is a graph which describes the major strains (ε_1) for all the values of the minor strain (ε_2) at the beginning of localized necking. Normally, it is difficult to determine a FLD due to the special equipment required, and the time needed. [3]

3. GTN MODEL

Gurson-Tvergaard-Needleman model says that local damage is due to nucleation, growth, and subsequent coalescence of voids inside the material. These mechanisms are responsible for a resistance loss which in turn, gradually leads to the failure. The equation 1 indicates the model. [1]

$$\Phi = \frac{q^2}{\sigma_y^2} + 2q_1 f^* \cosh\left(\frac{-3q_2 p}{2\sigma_y}\right) - (1 + q_3 f^{*2}) = 0 \quad (1)$$

where f*(*f*) is the damage function of the micro-void volume fraction or porosity (*f*).

Tvergaard considered the constants as $q_1 = 1.5$, $q_2 = 1$ and $q_3 = q1^2$ for the void volume fraction and pressure terms. q is the effective stress of the macroscopic Cauchy stress tensor and σ_y describes the hardening of a fully dense matrix material. The damage model considers three main phases of damage evolution including nucleation (N), growth (G) and coalescence (C) [1]:

$$df = df_N + df_G + df_C \quad (2)$$

The nucleation of micro-voids is expressed by [1]:

$$df_N = \left(\frac{f_N}{S_N\sqrt{2\pi}}\right)\exp\left\{-\frac{(\bar{\varepsilon}^p - \varepsilon_N)^2}{2S_N^2}\right\} d\bar{\varepsilon}^p \quad (3)$$

The normal distribution of the nucleation strain has a standard deviation of SN, a mean value of ε_N and nucleate voids with a volume fraction of f_N. Growth of the present voids is based on the apparent volume change and the law of conservation of mass, and is expressed as [1]:

$$df_G = (1-f).(d\varepsilon_{11}^p + d\varepsilon_{22}^p + d\varepsilon_{33}^p) \quad (4)$$

Finally, regarding the coalescence and final material failure, the modification of the yield condition is introduced through the function f*(f) specified by Tvergaard [1]:

$$\begin{cases} f^* = f & f < f_c \\ f^* = f_c + \delta(f - f_c) & f \geq f_c \end{cases}$$

* *Intsitute of Applied Mechanics, University of Miskolc*
** *Intsitute of Applied Mechanics, University of Miskolc*
*** *Institute of Machine and Product Design, University of Miskolc*

With:

$$\delta = \frac{(f_u^* - f_c)}{(f_f - f_c)} \qquad f_u^* = \frac{1}{q_1}$$

Table 1 The initial values of GTN parameters according to the literature. [3]

References	q_1	q_2	ε_N	S_N	f_0	f_F	f_N	f_C	Material	Comment
Bauvineau et al. (1996)	1.5	1	-	-	0.002	-	-	0.004	CMn steel	
Decamp et al. (1997)	1.5	1	-	-	0.0023	0.225	-	0.004	CMn steel	Uniaxial tensile test at 300°C on axisymmetric notched specimens
Siegmund et al. (1998)	1.5	1	0.3	0.1	0.0025	-	0.02	0.021	E460 steel	
Schmidt et al. (1997)	1.5	1	0.3	0.1	0	0.212	0.002	0.06	Ferritic steel base	Uniaxial tensile test at ambient temperature
	1.5	1	0.3	0.1	0	0.197	0.002	0.04	HAZ Ferritic	
	1.5	1	0.3	0.1	0	0.189	0.012	0.03	Austenitic steel cladding CMn steel	
Skallerad and Zhang (1997)	1.25	1	0.3	0.1	0.0003	0.15	0.006	0.026	CMn steel	Tensile test
Benseddiq and Imad (2008)	1.5	1	0.3	0.1	~0	~0.2	0.002-0.02	0.004-0.06		

4. MATERIAL AND METHODS

4.1. Material

Aluminum alloy 6061 was selected as the sample test. Table 2 lists the mechanical properties of the studied Aluminum alloy.

Table 2 Mechanical properties and thickness of Al6061 properties (heat treated).

Yield Stress (MPa)	~240
Tensile strength (MPa)	~260
Elongation (%)	~9-10
Hardness	85 HB
thermal expansion	23x10e-6 1/K
modulus of elasticity	~70 GPa
poisson ratio	0.35
density	2700 kg/m^3
thermal conductivity	~180W/mK

4.2. What is 6061 Aluminum?

6061 aluminum, also known as Alloy 61S, is a precipitation-hardened aluminum alloy, containing magnesium and silicon as its major alloying elements. Aluminum 6061 is one of the most commonly extruded alloys. It also has good weldability. 6061 aluminum is available in pre-tempered grades, including 6061-O, 6061-T, and 6061-F. The economical price, lightweight, high strength and versatility make alloy 6061 a popular material in CNC machining services to make precision aluminum machined parts for a host of industries.

4.2.1 6061 Aluminum Applications

Aircraft wings and fuselages, boats, automotive parts, flashlights, cans, fishing reels, firearms, forgings, bicycle frames and parts, etc.

Here is a comparison between A380 and 6061 aluminum in multiple aspects, including composition, physical properties, mechanical properties, and more. [4]

Table 3 Chemical composition of Al6061 properties

	6061 Aluminum
Aluminum (%)	95.9 - 98.6
Chromium (%)	0.04 - 0.35
Copper (%)	0.15 - 0.4
Iron (%)	0 - 0.7
Magnesium (%)	0.8 - 1.2
Manganese (%)	0 - 0.15
Nickel (%)	0
Silicon (%)	0.4 - 0.8
Tin (%)	0
Titanium (%)	0 - 0.15
Zinc (%)	0 - 0.25
Residuals (%)	0 - 0.15

Table 4 Physical and Thermal Properties of Al6061

	6061 Aluminum
Density (g/cm3)	2.7
Melting Completion (℃)	650
Melting Onset (℃)	580
Thermal Conductivity (W/m-K)	170
Thermal Expansion (µm/m-K)	24

Table 5 Mechanical Properties of Al6061

	6061 Aluminum
Elongation at Break, %	3.4 - 20
Fatigue Strength, MPa	58 - 110
Shear Modulus, GPa	26
Shear Strength, MPa	84 - 210
Ultimate Tensile Strength, MPa	130 - 410
Tensile Tensile Strength, MPa	76 - 370

Example: **AA6061**, used in car steering knuckles for instance, has an average tensile strength of 383 MPa and elongation 10.7%. The alloy was optimized by adding minor quantities of zirconium, zinc and copper. [5]

Table 6 Mechanical Properties of Al6061 with relation to temperature.

Temperature K	Elastic Modulus GPa	Poisson's Ratio	Thermal Expansion 10^{-6}/K	Thermal Conductivity W/m K	Specific Heat J/kg K
10	76.5951	0.3239	0.2525	14.3824	1.5609
20	76.5621	0.3240	0.5045	28.4645	8.8829
30	76.4967	0.3242	0.9477	41.0270	33.4402
40	76.4011	0.3243	1.7028	52.2049	81.9529
50	76.2777	0.3245	2.8316	62.1332	149.1508
60	76.1285	0.3248	4.3375	70.9469	223.9242
70	75.9555	0.3250	6.1652	78.7811	297.9033
80	75.7608	0.3253	8.2007	85.7707	368.3660
90	75.5463	0.3255	10.2179	92.0509	433.5356
100	75.3137	0.3258	11.8261	97.7565	492.5810
110	75.0647	0.3262	13.1962	103.0226	545.6162
120	74.8011	0.3265	14.3611	107.9842	593.7009
130	74.5243	0.3268	15.3513	112.7788	637.9319
140	74.2358	0.3271	16.1946	116.8674	677.6165

4.3. Tensile test simulation results

Assuming the Tvergaard coefficients being fixed, the model parameters were adjusted by applying an uniaxial tensile test.

In particular, the load vs. displacement curve during a tensile test on a sheet specimen must be employed to optimize the comparison between the numerical results and the experimental ones, and consequently to achieve the desired material characterization.

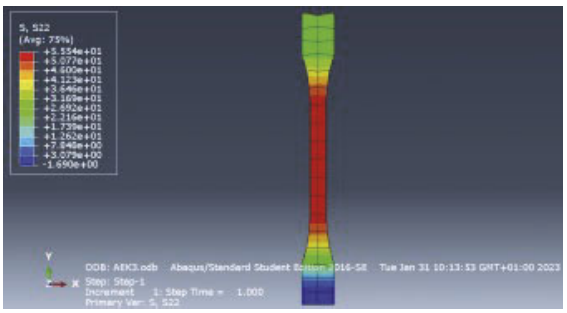

Fig.1 Elastic deformation

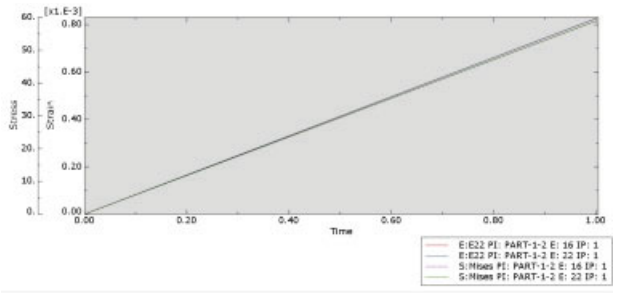

Fig.2 Stress x Time

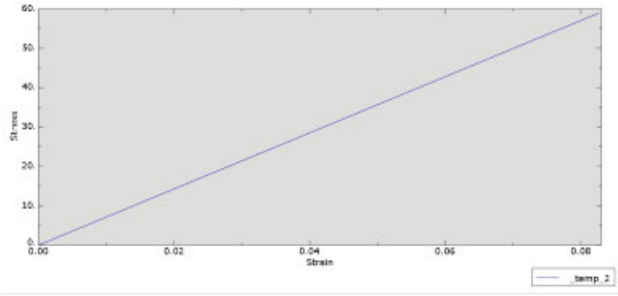

Fig.3 Stress x Strain

4.4. Perspectives

The main goal is to determine the GTN parameters for an Aluminum alloy with industrial applications.

Assuming the Tvergaard coefficients being fixed, the model parameters were adjusted by applying an uniaxial tensile test.

In particular, the load vs. displacement curve during a tensile test on a sheet specimen has been employed to optimize the comparison between the numerical results and the experimental ones, and consequently to achieve the desired material characterization. [2]

The value of Ɛ has been fixed equal to 0.0002 [2]
From [7] Modeling and simulation. Temperature dependent material properties for Aluminum 6061.

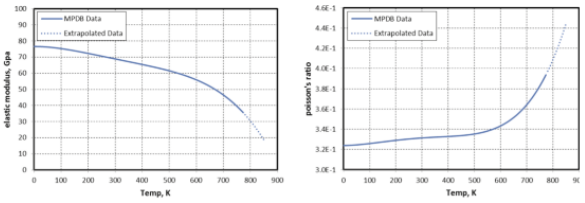

Fig.4 a) Elastic Modulus; b) Poisson's Ratio

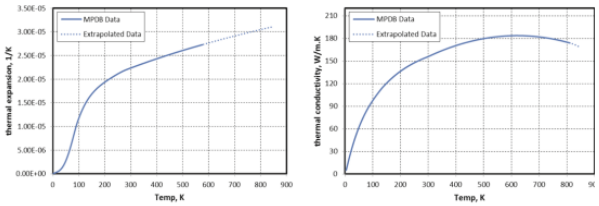

c) d)

Fig.5 ; c) Thermal Expansion; d) Thermal Conductivity

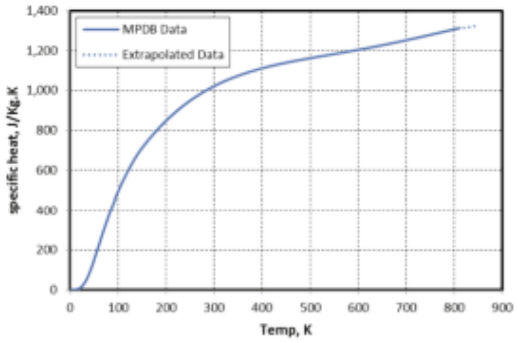

c)

Fig.6 e) Specific Heat.

Figure 4, 5 and 6: Properties include a) Elastic Modulus; b) Poisson's Ratio; c) Thermal Expansion; d) Thermal Conductivity; and e) Specific Heat.

Table 7: material properties for Aluminum 6061 at room temperature.

Density, kg/m^3	2700
Elastic Modulus, GPa	68.9
Poisson's ratio	0.33
Thermal conductivity, W/mK	220
Specific heat, J/kgK	904
Thermal Expansion coefficient, $10^{-6}K^{-1}$	23.6

Table of Temperature Dependent Material Properties for Aluminum 6061
Data is taken from MPDB material database software [6]

6. REFERENCES

[1] M. Abbasi, "Identification of GTN model parameters by application of response surface methodology," ScienceDirect, Procedia Engineering10 pp. 415–420, 2011, doi:10.1016/j.proeng.2011.04.070

[2] L. Fratini, "Material Characterization for the Prediction of Ductile Fracture Occurrence: An inverse approach," in Journal of Materials Processing Technology, Volume 60, Issues 1-4, 15 June 1996 ed. Palermo, Italy: 1996, pp. 311–316. doi:10.1016/0924-0136(96)02347-3

[3] C. Yassine, "Determination of GTN Parameters of Sent Specimen During Ductile Fracture," MultiScience – XXXIII. MicroCAD International Multidisciplinary Scientific Conf., Miskolc, Hungary, 2019, ISBN 978-963-358-177-3.

[4] DCM Diecasting-Modul - A380 Aluminum vs 6061, What's the Difference - What is A380 Aluminum | Diecasting-mould

[5] Aluminium Alloys in the Automotive Industry: Handy Guide – Aluminium Insider [Online].Available:aluminiuminsider.com/aluminium-alloys-automotive-industry-handy-guide

[6] I. JAHM Software Inc. (1998) Mpdb material database software. [Online]. Available: https://www.jahm.com/pages/about mpdb.html

[7] Tuning Johnson-Cook Material Model Parameters for Impact of High Velocity, Micron Scale Aluminum Particles | Semantic Scholar